AIMS Biophysics, 5(2): 97–124.
DOI: 10.3934/biophy.2018.2.97
Received: 21 January 2018
Accepted: 02 April 2018
Published: 23 April 2018

http://www.aimspress.com/journal/biophysics

Review

Insights into cell motility provided by the iterative use of mathematical modeling and experimentation

Juliet Lee*

Department of Molecular and Cell Biology, The University of Connecticut, 91 N. Eagleville Road, Storrs, CT 06269, USA

* **Correspondence:** Email: juliet.lee@uconn.edu; Tel: +8604864332.

Abstract: Cell movement is a complex phenomenon that is fundamental to many physiological and disease processes. It has been the subject of study for more than 200 years, and yet we still do not fully understand this process. Cell movement consists of four steps; protrusion and adhesion formation at the front followed by contractile force generation and detachment at the rear. Much is known about the molecular mechanisms underlying these steps however, it is not clear how they are integrated at the cellular level. Part of the problem is the incorporation of a vast amount of molecular and biophysical data into a basic working model of motility. A promising solution to this problem is the combined approach of mathematical modeling and experimentation, using the fish epithelial keratocyte as a model system. The goal of this review is to illustrate, using examples, how the reciprocity between experimentation and modeling can provide new insights into the mechanism of cell motility. Several modeling approaches are described including: conceptual models, "bottom-up" models based on molecular dynamics, and "top-down" models that consider cell shape and movement. The Graded Radial Extension (GRE) model forms the basis of a several mathematical models, from a simpler 1D model that links actin filament dynamics to cell shape, to more complex 2D and 3D simulations of keratocyte movement. Together these models suggest that cell movement emerges from the mechanical interaction between different sub-processes of motility, namely, the treadmilling actin meshwork, the plasma membrane, adhesion turnover and contractile force generation. In addition, the feedback regulation between these sub-processes is important for the robust, self-organizing nature of movement.

Keywords: cell motility; cytoskeleton; keratocyte; mathematical models

1. Introduction

The quest to understand how cells move is an old one, beginning more than 200 years ago with the observations of Anton Leeuwenhoek. Interest in this process has been sustained over the centuries, because it is recognized as playing a key role in physiological and disease processes. Cell motility is essential for normal embryonic development, efficient wound healing and for the immune response to infection and injury. Unregulated cell motility is one of the major reasons why cancer metastasis can be lethal. Despite the long history of cell motility research, it remains one of the outstanding questions in cell biology. The reason for this is that it is a highly complex phenomenon involving the integration of numerous molecular interactions over multiple size scales, ranging from the nanometer to millimeter scale. In addition, these processes must be coordinated spatially and temporally. Over the past several decades, much has been learned about the molecular basis of cell motility [1]. However, it is still not clear how this "molecular machinery" leads to movement at the cellular level. Part of the reason for this is the predominately reductionist approach that has been taken to studies of cell motility [2]. Unlike the dismantling of a complex machine to deduce how it works, the identification of the key molecules involved in cell motility has not automatically increased our understanding of movement at the cellular level. Over the past 30 years, mathematical modeling of cell motility has become increasingly important in furthering our understanding of this process. As cell biological studies continue to provide more molecular detail, mathematical modeling has provided a means of organizing large complex data sets into a quantitative "framework". This enables the researcher to test assumptions and refine hypothesizes. Perhaps the most valuable aspect of mathematical models is their ability to make predictions that can then be tested by experimentation, the results of which can be used to revise the original model.

The purpose of this review is to describe how the iterative use of experimentation and modeling has provided insights into the movement of fish epithelial keratocytes. This cell type is uniquely suited to this purpose, since their simple geometric shape and rapid, gliding mode of movement greatly simplifies the task of linking molecular scale events to whole cell movement. A short introduction to cell motility will be given, followed by a description of conceptual models first, then mathematical models will be summarized in approximately chronological order (Table 1). The emphasis of this review will be on models that relate molecular mechanisms to the mechanics of motility, and where there is a direct link between modeling and experimentation. Models of the signaling mechanisms involved in movement or the development of cell polarity will not be included. Note also that this review will not include details about the mathematical methods used, or how they were constructed. Excellent reviews of both mathematical approaches to modeling [3] and models of keratocyte motility are available [4–6]. In addition, models of keratocyte motility from the physics literature that will not be discussed here include: Oetz and Schmeiser, 2012 [7]; Adler and Givli, 2013 [8]; Recho et al., 2013 [9]; Tjhung et al., 2014 [10]; Ambrosi and Zanzottera, 2016 [11]; and Raynauld et al., 2016 [12]. Lastly, in the discussion section, an overview of the contributions that mathematical modeling has made to our understanding of cell motility will be given, followed by some suggestions of future directions.

Cell crawling along a surface is a complex, highly coordinated, physical process that at the sub-cellular level involves cycles of protrusion and adhesion at the front edge, followed by contractile force generation and detachment at the rear. At the molecular level, each of these motile sub-processes is underpinned by the dynamic behavior of the actin cytoskeleton and its associated proteins [13,14].

Protrusion occurs at the very edge of the lamellipodium due to the rapid polymerization of actin filaments. This generates an outward "pushing" force against the plasma membrane by acting as a thermal ratchet. Thermal fluctuations at the actin filament plus (or barbed) end allow the intercalation of actin monomers, thus lengthening the filament [15]. The rate and location of actin polymerization is controlled by many different actin binding proteins [13]. In response to an external signal, activation of nucleation promoting factors (NPFs) and subsequently the Arp2/3 complex initiates the branching growth of a dense actin meshwork within a narrow 1–2 μm band just behind the leading edge [16]. Within seconds, free actin filament plus ends are capped as their relative position shifts further behind the leading edge. The activity of capping proteins together with severing and actin depolymerizing proteins maintains a high rate of polymerization at the leading edge through a process termed funneled treadmilling [17]. This process allows fast moving keratocytes to assemble a new lamellipodium every minute. To stabilize the lamellipodium, actin binding proteins, such as filamin, α-actinin, and tropomyosin crosslink actin filaments, thus increasing cytoskeletal rigidity and providing a solid base from which the leading edge can protrude.

The formation and disassembly of cell-substratum adhesions is essential for protrusion and retraction, respectively. Adhesions are multi-molecular complexes that link proteins of the extracellular matrix to the cytoskeleton intracellularly. In most vertebrate cells, adhesions consist of many types of integrin adhesion receptors together with other structural and signaling proteins [18]. New adhesions form at the advancing edge where they anchor the lamellipodium to the substratum. These nascent adhesion complexes are composed of relatively few structural and signaling proteins but as the cell moves over them, they enlarge and become molecularly more complex. In addition, their molecular linkage to the cytoskeleton becomes reinforced, which enhances the transmission of biochemical and mechanical signals between the cell and its environment [19]. Adhesion reinforcement has been likened to the engagement of a molecular clutch [19,20], which allows cytoskeletal contractile forces to be exerted on the substratum as traction stress. Once adhesions have "matured" into focal adhesions they provide the strongest attachment to the substratum, and are the sites where large traction stresses are generated. As focal adhesions reach the rear cell edge they must disassemble so that detachment can occur, otherwise they will hinder forward movement.

Myosin II dependent contractile force generation is an integral part of cell motility [21]. At the leading edge, myosin II minifilaments associate with actin, are sparse [16], and generate weak isotropic contractile forces. These are necessary for the reinforcement of nascent adhesions, and for stabilizing adhesions beneath the extending lamella. The transmission of weak contractile forces in this region results in the generation of traction stresses, which allow the cell to "grip" the substratum. These are thought to represent "propulsive" tractions that "pull" the cell body forward. Further back, myosin II minifilaments coalesce into larger filaments, to form new stress fibers at the rear of the cell, where they generate the largest contractile forces. These are believed to inhibit protrusion, while facilitating rear detachment. In most cell types, contractile forces are believed to aid in "ripping" up adhesions [22]. However, contractile force has been implicated in other mechanisms of detachment, such as: The activation of stretch-activated calcium channels [23], the activation of proteolytic enzymes [24], and force-induced increase in the dissociation constants of adhesion components [25]. This spatial organization of contractile forces is important for maintaining protrusion at the front and retraction at the rear, so that repeated cycles of protrusion and retraction can occur. In keratocytes, and lamellar fragments this structural organization of actin and myosin II is maintained due to its self-organizing activity of [26].

Moving cells respond to a variety of signals in their environment [27]. Diffusible signals guide leukocytes to their targets via the process of chemotaxis, while the movement of other cell types can be guided by immobilized signals in the extracellular matrix (ECM). The mechanical properties of the cell's environment such as surface adhesiveness, texture, stiffness and porosity can also provide guidance cues [28]. For example, increasing stiffness of the ECM at the edge of a wound guides fibroblasts and epithelial cells towards it by the process of durotaxis [29]. All of these signals trigger signaling pathways that converge on the Rho family of GTPases that play a pivotal role in the regulation of cell motility [27]. The GTPases Cdc42 and Rac are activated first at the front of the cell. They induce the formation of lamellipodia by activating the Arp2/3 complex via their downstream effectors WASp and WAVE, respectively. At the same time, these GTPases reduce contractility by decreasing the phosphorylation of both myosin light chain kinase (MLCK) and the myosin II heavy chain. Activation of the Rho GTPase occurs downstream of Cdc42 and Rac, and through its downstream effector Rho kinase, it inhibits myosin light chain phosphatase, thus increasing contractility. Its activity is highest at the rear where it facilitates retraction and inhibits protrusion. Rho GTPase activation also promotes the formation of mature focal adhesions and stress fibers. Thus the sequential and antagonistic activity of Rac and Rho GTPases controls the temporal and spatial organization of cytoskeletal function.

Different cell types display a variety of characteristic shapes and modes of movement, despite the highly conserved nature of the cytoskeleton. Fibroblasts tend to be triangular in shape with one broad lamella at the front that tapers to a narrow tail at the rear (Figure 1). Their movement is slow and discontinuous, consisting of a period of protrusion at the front followed by a separate phase of retraction at the trailing edge [30]. In contrast, white blood cell types such as leukocytes and macrophages exhibit a more rapid type of movement, in which the front edge forms several competing protrusions, often extending in different directions, until one of them becomes larger and dictates the direction of movement [31] (Figure 2). The most efficient, and rapid type of movement is exhibited by the fish epithelial keratocyte [32] Figures 4C, D. These cells maintain a simple semicircular or "fan" shape and a continuous, gliding mode of movement. Unlike many other cell types whose movement can be described as a random walk [33] keratocytes can maintain their shape and direction of movement for several minutes at a time.

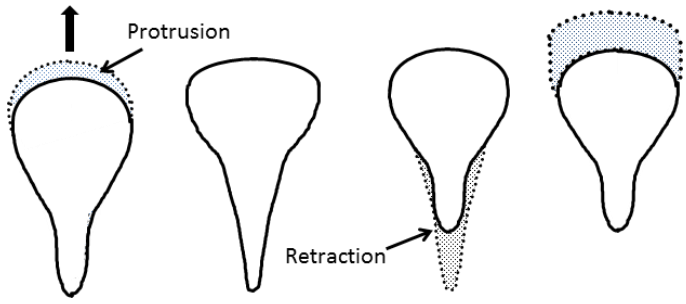

Figure 1. Diagram of a typical fibroblast exhibiting slow, discontinuous movement in the direction indicated (large arrow). A phase of protrusion (grey area) is shown, followed by inhibition of protrusion due to the stuck "tail" at the rear. Retraction at the rear (grey area) is followed by a surge of protrusion at the front (stippled area).

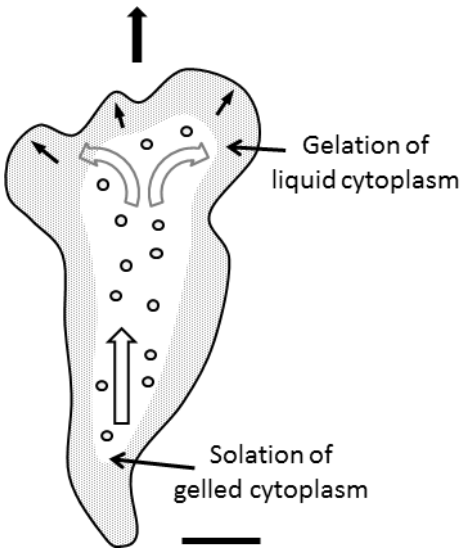

Figure 2. Diagram of an amoeboid cell displaying cytoplasmic streaming in the directions indicated (open arrows). A region of gelled cytoplasm is shown at the periphery of the cell (shaded region) and a liquid, solated cytoplasm, containing intracellular vesicles (shaded circles) is seen in the center of the cell. Three protruding regions (small arrows) are shown at the front of the cell. Scale bar = 5 μm.

2. Approaches to modeling cell motility

One of the major challenges to understanding motility is the integration of molecular dynamics, cytoskeletal function and biomechanics with cell shape and movement. Although a variety of models, both conceptual and mathematical have been proposed over the past several decades, this task is not yet complete. Given the complex, multifaceted nature of cell movement it is not surprising that this is so. There have been a number of obstacles to developing a complete model of motility. The variability in shape and mode of movement that exists between different cell types complicates the process of deriving a basic mechanism underlying cell motility. In addition, models of motility vary in their degree of complexity, approach and aspect of movement being modeled [3]. For example, a relatively simple 1D model considers the movement of the amoeboid sperm from the nematode *Ascaris suum* as a single cytoskeletal filament spanning the front to rear of the cell [34]. At the other extreme, a highly complex 3D model of cell movement treats the cytoskeleton as a two-phase interpenetrating flow of a liquid cytosol and a visco-elastic solid cytoskeleton [35]. In general, there are two broad categories of model, the "top-down" approach that focuses on the shape and movement of the whole cell [36] and the "bottom up" approach whose emphasis is on the molecular mechanisms underlying cell motility [37]. Ultimately, a combination of both approaches is likely to provide a more complete model of motility. For example, a more recent approach to modeling motility is the development of "integrative" or multi-scale models that are a combination of top-down and bottom-up approaches. The choice of the fish epithelial keratocyte for both cell biological studies and mathematical modeling is particularly useful, because its simple shape and gliding mode of movement facilitate linking molecular scale processes to cell shape and speed.

Table 1. Summary of conceptual and mathematical models of cell motility.

Model name/type/cell system/authors	Hypothesis or Goal	Prediction	Experimental support	Insight or Outcome
Fountain flow model/conceptual [38]	Increased hydrostatic pressure drives cytoplasm forward to push out the front.	n/a	Forward streaming of cytoplasmic vesicles. Gel-sol transitions of actin and gelsolin *in vitro*.	Provides a conceptual framework for relating molecular mechanisms to the material properties of the cytoplasm.
Retraction induced spreading (RIS)/conceptual/fibroblasts [39]	Cytoskeletal tension promotes retraction but inhibits protrusion.	n/a	Rapid increase in area protruded following retraction.	Accounts for discontinuous mode of fibroblast motility. Suggests cytoskeletal tension may coordinate protrusion and retraction.
Retrograde flow/conceptual/fibroblasts [40]	Treadmilling caused by actin polymerization at front of lamellipodium and depolymerization at its rear.	n/a	Retrograde flow of surface particles, actin arcs, photo-bleached lines.	Provides a conceptual framework for how actin filament dynamics powers protrusion.
GRE model/kinematic 2D/keratocytes [41]	Protrusion occurs in a graded manner perpendicular to the cell margin. Retraction is also graded and perpendicular to cell edge.	Circumferential motion along front and rear cell margins.	Circumferential motion of lamellar folds and curved retraction fibers. Curvature of photo- lines in resorufin-actin.	Accounts for the constant size, semicircular shape and direction of movement. Provides a basis for future mathematical models.
1D model/keratocytes [37]	Shape of extending edge depends on rate of actin polymerization.	Shape of leading edge, matches model prediction well if low capping rates are assumed.	Fluorescence intensity measurements from images of fixed cells.	Provides information on the molecular basis for protrusion according to the GRE model.
2D model/keratocytes [42]	The shape of the leading edge is related to cell speed.	Model describes shape and speed of 93% of all observed keratocyte shapes using only 2 parameters, cell area and aspect ratio.	Large scale analysis of cell shape and speed.	Links molecular mechanisms to cell shape and speed.

Continued on next page

Model name/type/cell system/authors	Hypothesis or Goal	Prediction	Experimental support	Insight or Outcome
2D multiscale model/keratocyte lamellipodial fragments [43]	To integrate actin filament dynamics, protrusion, adhesion, contractility and retraction into a multiscale model of keratocyte motility.	Reproduces keratocyte-like movement, of a lamellipodial fragment Predicts turning of keratocytes after local photorelease of caged thymosin β4.	Observations of moving lamellipodial fragments turning behavior of keratocytes following photorelease of caged thymosin β4.	First multiscale model to integrate motile sub processes into whole cell movement.
2D integrative model/ keratocytes [44]	Cell shape arises from mechanical feedback between polymerizing actin, myosin dependent retrograde flow, membrane tension and adhesion strength.	Simulations match experimental observations in terms of shape, speed, retrograde actin flow, distribution of myosin II and adhesions on surfaces of low, medium and high adhesiveness.	Observations of keratocyte shape and speed. Immunofluorescence distribution of myosin II and adhesions on surfaces of low, medium and high adhesiveness.	The mechanism of cell shape determination depends on substratum adhesiveness.
Integrative 3D biomechanical model/keratocytes [35]	The 3D shape and mode of cell movement can be explained by a low Reynolds number hydrodynamic finite element model, *Cytopede*.	Simulations match experimental observations. Predicts the interconversion between a fibroblast and keratocyte shape and movement depending on rear adhesion and how much of the leading edge participates in protrusion.	Observations of moving keratocytes and fibroblasts.	The first 3D model based on the biophysical properties of the cytoplasm. Can account for the interconversion between fibroblast and keratocyte movement.

Continued on next page

Model name/type/cell system/authors	Hypothesis or Goal	Prediction	Experimental support	Insight or Outcome
Four minimal 2D models/keratocytes [45]	Cell shape and speed is underlain by one or more basic mechanisms, acting alone or in combination.	Three* minimal models predict the shape and movement of keratocytes. *The 4th myosin II based model does not.	Some experimental support for each of the minimal models. See reference for details.	The shape and mode of keratocyte movement is robust because redundant mechanisms exist that can compensate for each other.
2D integrative model/amoeboid sperm of *Ascaris suum* [46]	The "push-pull" hypothesis [47] higher pH leads to crosslinking of MSP to push at cell front. Lower pH leads to disassembly of MSP to pull at rear.	Reproduces the shape and mode of *Ascaris* sperm movement. Predicts effects of decreasing intracellular pH or increasing substratum adhesion strength.	Observations of *Ascaris* sperm movement and the effects of decreasing intracellular pH or increasing substratum adhesiveness.	Provides evidence that different molecular mechanisms can reproduce the same mechanical principles that underlie keratocyte movement.
Top-down 2D models of various cell types [36]	Various cell shapes and types of movement arise from differences in regulation of motile sub processes.	Reproduces the shape and motion of different cell types. Predicts the interconversion between them.	Observation that inhibition of SAC mediated feedback between front and rear converts keratocytes to a fibroblastic mode of movement.	Different cell shapes and modes of movement can arise from alterations in the feedback control of protrusion, retraction adhesion and contractility.

2.1. Early conceptual models of cell motility

The purpose of conceptual models is not simply to describe an observation but to use it to form initial hypotheses. This may be regarded as the first approach to the development of more quantitative models. One of these early conceptual models was based on the observation of amoeboid cell movement, in which granular streams of cytoplasm could be seen moving toward the front of the cell (Figure 2). This process referred to as "fountain" flow was thought to be generated by increased hydrostatic pressure due to myosin II dependent contraction at the cell rear [38]. Such "squeezing" at the rear was believed to generate a protrusive force by forcing the cytoplasm forward. Repeated cycles of protrusion and retraction were proposed to result from the liquefaction of solid cytoplasm at the retracting edge and "gelling" of cytoplasm at the front edge. This model was supported by the finding that calcium dependent activation of an actin binding protein, gelsolin could "solate" or decrease the viscosity of the cytoplasm by severing actin filaments [48]. Conversely, decreased gelsolin activity together with the function of the actin filament crosslinkers, filamin and myosin II can increase cytoplasmic viscosity.

Fibroblasts were another cell type that was the focus of early studies of cell motility, since they were relatively easy to obtain and culture in the laboratory. It was noticed that the rate of protrusion decreased as the cell became elongated, until detachment occurred abruptly at the rear (Figure 1). Retraction at the rear was typically followed by a surge of protrusion, which was termed retraction-induced spreading (RIS) [39]. One explanation for this phenomenon was that increasing cytoskeletal tension progressively inhibits protrusion, until it is sufficient to trigger retraction. The subsequent release of tension allows protrusion to resume. The presumption of the RIS model is that the level of cytoskeletal tension acts to coordinate cycles of protrusion and retraction. Therefore, this model was one of the earliest to imply cytoskeletal tension is involved in coordinating protrusion with retraction.

In the early 1970s, time-lapse, light microscope recordings of cell movement showed that particles and other surface features tend to be swept inward from the front of the cell to a region in front of the cell body. This movement, termed retrograde flow [40], was believed to be part of the molecular mechanism that drives cell movement (Figure 3A). Cell motility research and associated conceptual models became focused on answering two related questions; what drives retrograde flow, and how does it relate to movement? One suggestion was that the treadmilling of long actin filaments in the lamella could act as a "conveyer belt" to move surface attached particles rearward if they were mechanically coupled to the actin filaments. If instead these particles were immobilized on the substratum, then actin filament growth would allow the front cell edge to protrude, while the relative position of the particles would remain stationary with respect to the substratum but move rearward with respect to the front edge (Figure 3B). However, experiments with the nerve growth cones from the sea slug *Aplysia* showed that myosin II dependent contractility was, indeed, the driving force for the retrograde flow of particles on the dorsal cell surface, not treadmilling [49]. This finding raised the question of how myosin II driven retrograde flow contributes to movement. According to one idea immobilizing retrograde flow could allow more of the newly polymerized actin to contribute to protrusion, instead of it being swept rearward. Photoactivation experiments with moving keratocytes showed this to be correct [50]. When a bar shaped fluorescent mark was made in a subset of actin filaments on the lamella, it remained stationary with respect to the substratum, so that all the newly polymerized actin could contribute to protrusion. Another role for myosin II dependent retrograde flow is to allow cells to "grip" the substrate via cell-substratum adhesions, and thus pull the cell body forward. This possibility was supported by the pioneering work of A. Harris in 1980 who showed that motile fibroblasts attached to flexible silicone films could pull them inward in a myosin II dependent manner, causing the film to wrinkle [51]. This represented the first use of a "traction force" assay to detect the contractile forces that moving cells exert on the surface. Subsequently, different types of traction force assay have allowed quantification of the forces cells use for movement [52]. The significance of this new technological advance was that it allowed researchers to relate molecular mechanisms to the mechanics of motility, for the first time. As a result, new conceptual models were developed. For instance, the "frontal towing" model proposed that small nascent adhesions at the leading edge of moving cells provide large "propulsive" tractions that pull the cell forward, while high traction stresses at the rear edge represent a passive drag force [53,54].

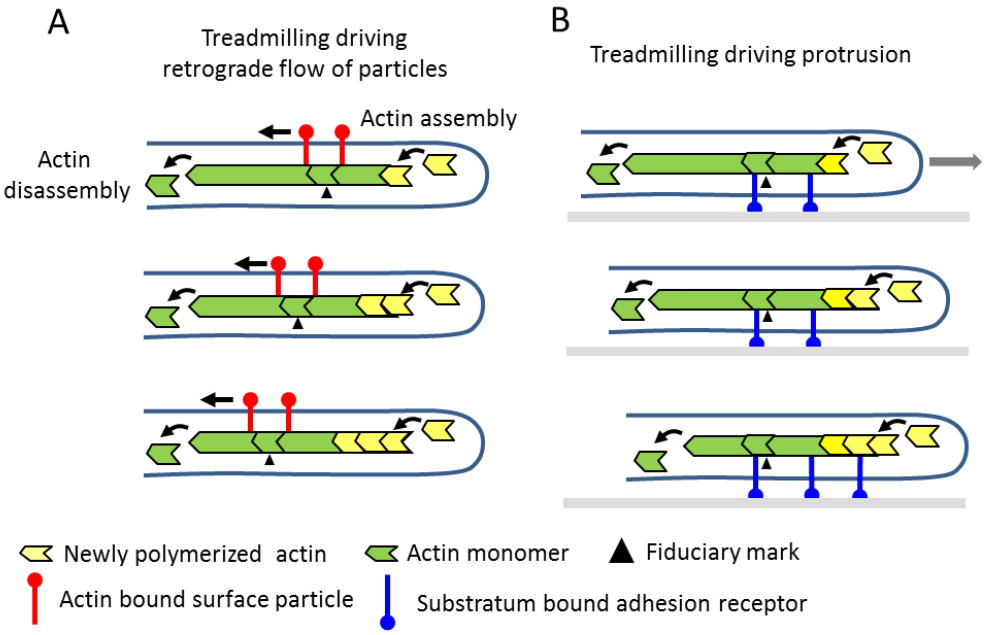

Figure 3. Diagrams illustrating how treadmilling of actin filaments can drive the retrograde flow of surface particles or protrusion. A: A treadmilling actin filament (green) is shown with actin monomers being added at the plus (barbed) end (yellow symbols) while monomers are lost at the minus (pointed) end. Two surface particles bound to the actin cytoskeleton (red symbols) are indicated by a fiduciary mark (black triangle). The relative position of the surface particles moves rearward (small arrows) with respect to the substratum and the leading edge. Note that there is no protrusion, because retrograde flow is not opposed by attachments to a substratum. Thus all new polymerization contributes to retrograde flow. B: A treadmilling actin filament as shown in A. Here the actin filament is anchored to the substratum by adhesions (blue symbols) which oppose retrograde flow. Note that the position of a single actin monomer (black triangle) does not change with respect to the substratum but it moves rearward with respect to the leading edge. This is because all the newly polymerized actin contributes to protrusion (grey large arrow).

2.2. Mathematical models

Since the 1980s, cell motility research has focused mostly on identifying the molecular mechanisms underlying cell motility. This trend was paralleled by the development of mathematical models that included increasing amounts of molecular detail. Although many of these provided a better understanding of a defined set of molecular processes, they did not reveal a general organizing principle that governs the integration of molecular scale processes to the movement of an entire cell. It was not until the early 1990s, when studies of the fish keratocyte [32,41] provided a foundation for more "integrative" models of motility. It also marked the time of increased collaboration between mathematicians and cell biologists, which has been sustained over almost three decades. A major collective insight provided by this work is that cell motility is an emergent property arising from a multitude of molecular interactions, which cannot simply be inferred from molecular detail alone.

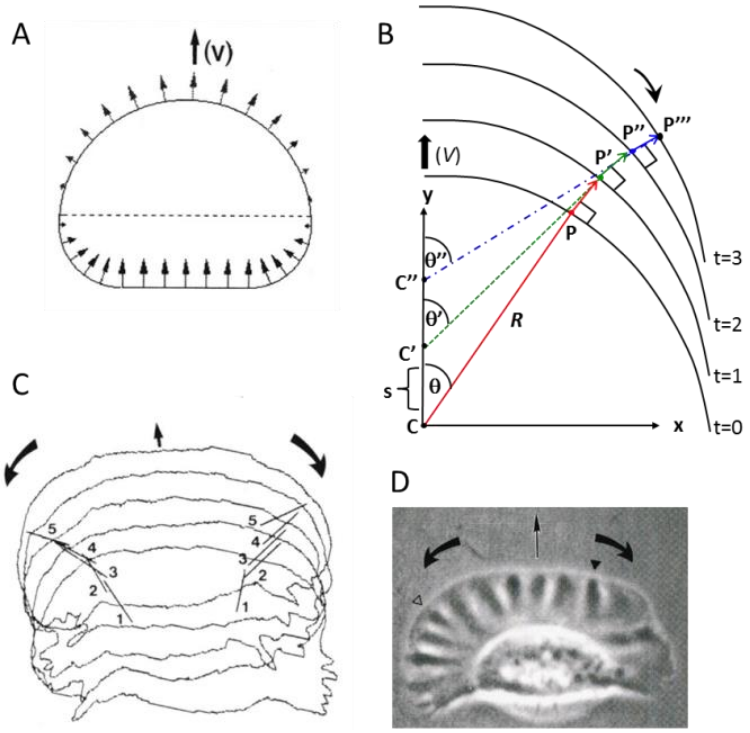

Figure 4. Illustration of graded radial extension and retraction together with experimental evidence for circumferential motion. A: Diagram of a keratocyte moving with a velocity (*V*). Arrows represent graded radial extension at the front of the cell and graded radial retraction at the rear. B: Kinematics of a point, P on the cell margin undergoing graded radial extension that results in circumferential motion. C: Cell outlines of a moving keratocyte (small arrow) taken every 12 seconds showing the change in position with respect to the substratum of the lamellar ridges seen in D. Their resultant circumferential motion with respect to the cell is indicated (curved arrows). D: Phase contrast image of the moving keratocyte shown in C. Lamellar ridges on the left (open triangle) and right side (closed triangle) were tracked. Their circumferential motion is indicated (curved arrows). Scale bar = 10 μm.

2.2.1. The Graded Radial Extension (GRE) model for keratocyte movement

Fish epithelial keratocytes offer a unique advantage over other cell types for relatinmolecular mechanisms to whole cell movement, because of their simple, semicircular shape and gliding mode of movement [32]. Therefore, the organization of cytoskeletal function within the frame of the cell remains unchanged for many minutes at a time. The constancy of keratocyte shape and motion is in stark contrast to other irregularly-shaped cell types such as leukocytes whose movement can be described as a random walk [33]. This observation raised the question of how keratocytes maintain their shape and constant velocity. The answer to this question lies in the assumption that protrusion occurs perpendicular to the adjacent cell margin and is graded such that the maximum rate occurs at the midline of the front cell edge and decreases to zero at the sides (Figure 4A) [32]. The GRE model predicted that the relative position of morphological features, such as lamellar folds (Figure 4D) would drift along the circumference of the cell in an anti-clockwise direction on the left side, and in a

clock-wise direction on the right side (Figure 4B). The relative motion of a point on the protruding cell margin may be calculated as follows. Consider an arbitrary point P on the right side of the front edge of a keratocyte moving forward with a velocity *V*. At t = 0, P lies on a semicircle of radius *R* (red, solid line) and origin C, at the center of a Cartesian coordinate system fixed with respect to the substratum. Points on this semicircle are given by $x^2 + y^2 = R^2$, where $0 \le x \le R$ and $0 \le y \le R$. At t = 1, the semicircle has moved a small distance, *s* (where $0 < s < R/10$) along the *y* axis such that its origin C has moved to C'. The radius *R* remains constant (green, dashed line). At t = 1, points on this semicircle are given by:

$$x'^2 + (y' - s)^2 = R^2 \quad (1)$$

In addition, P extends perpendicularly to the cell edge to its new position P' along straight line CP given by:

$$y = mx \quad (2)$$

Where $m = \tan(90° - \theta)$ and θ is the angle between CP and the y axis. The coordinates (x', y') of P' are given by the simultaneous solution of Eq 1 and Eq 2 to yield $x' = [ms + (R^2(1 + m^2) - s^2)^{1/2}]/(1 + m^2)$, and $y' = [m^2 s + m(R^2(1 + m^2) - s^2)^{1/2}]/(1 + m^2)$. The new angle that C'P' makes with the y axis is $\theta' = 90° - \arctan[(y' - s)/x']$. By repeating this calculation, the successive positions of P, P'' and P''' can be found at t = 2 and t = 3, with respect to the substratum and the cell. Note that the successive positions of P trace a curved trajectory with respect to the substratum in addition to moving along the circumference of the cell in a clockwise direction (curved arrow). As predicted, lamellar folds were found to exhibit circumferential motion relative to the cell frame (Figure 4C) [41]. Thus the GRE model defines the kinematics of protrusion and retraction that is necessary for the maintenance of keratocyte shape and constant forward motion.

2.2.2. A model that links actin filament dynamics to graded radial protrusion

The GRE model describes the kinematics of keratocyte movement, without making any assumptions about the molecular mechanisms involved. One of the first attempts to link actin filament dynamics to the graded rates of protrusion was developed by Grimm et al., in 2002 [37]. They found a graded distribution of actin filament density along the leading edge that is highest at the middle of the front edge and lowest at the sides. To determine how this gradient of actin filament density could give rise to graded radial protrusion rates, a 1D mathematical model was constructed that reflected the geometry and dynamics of actin filaments. It was assumed that the shape of the leading edge is directly related to the rate of actin polymerization, since it has been shown that the front of the lamellipodium is stationary with respect to the substratum [50]. In addition, actin filaments were modeled as branching at +35 ° or −35 ° with respect to the advancing edge, consistent with Arp2/3 dependent nucleation of actin filament growth. It follows from this that "mother" filaments on the left side would drift anticlockwise, with respect to the cell frame, while "daughter" filaments on the right would move in a clockwise direction. The model simulations resulted in curves representing the shape of the leading edge. By fitting results of simulations with measurements of actin density obtained experimentally, estimates of capping rates could be made. Surprisingly, it was found that the best match between theory and experiment was obtained with low capping rates ($\gamma \sim 0.1\ s^{-1}$), and when the difference in actin density between the middle and sides of the front edge is

large (Figure 5A). In contrast, high capping rates led to irregular, "flattened" actin density profiles, in which actin filament density varied very little between the middle and sides (Figure 5B). However, low capping rates are predicted to give rise to average filament lengths on the order of a few microns, which is in contrast to the very short filament lengths seen in ultrastructural studies [16]. This discrepancy between predicted and observed filament lengths has yet to be resolved. Nevertheless, this model demonstrates how actin filament structure and dynamics can be linked to cell shape. In addition, the model provides an explanation for graded rates of protrusion along the leading edge, and thus lendss support for the GRE model.

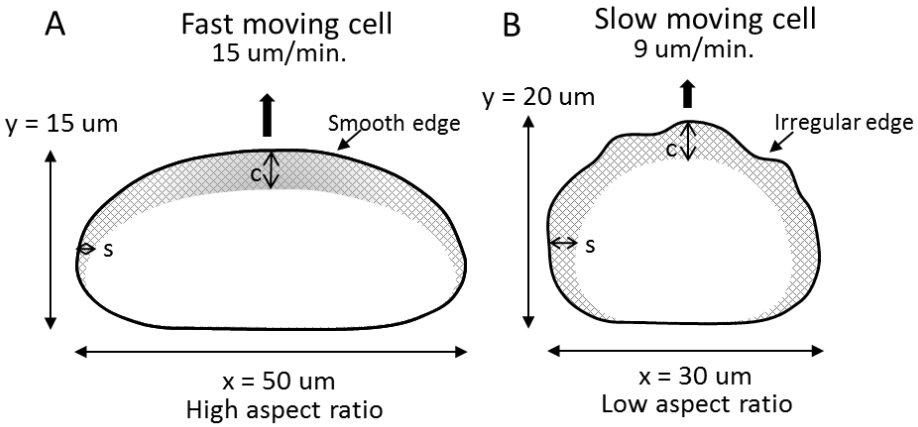

Figure 5. Diagrams of the shape and distribution of actin filament density at the leading edge of fast and slow moving keratocytes. A: Typical shape of a fast moving keratocyte with a smooth front edge and elongated along the x axis, perpendicular to the direction of movement (large, black arrow). Actin filament density is highest and widest at the center of the leading edge (C, double-headed arrow). Actin filament density and width decreases toward the rear lateral edges of the cell (S, double-headed arrow). The aspect ratio of this cell is high. B: Typical shape of a slow moving keratocyte with an irregular leading edge and more rounded in shape than A. Actin filament density and width at C is slightly greater than S, which corresponds to a low aspect ratio.

2.2.3. A 2D model that links actin filament dynamics to cell shape and speed

Keratocytes exhibit a range of shapes from fast moving fan-shaped cells to slow moving cells that resemble fibroblasts and move in a discontinuous manner [55]. Even between fan-shaped keratocytes there is some variation in shape. A quantitative analysis of a large number of keratocytes revealed that faster moving cells tend to be "canoe-shaped" with a smooth outline and a high aspect ratio (Figure 5A). Slower moving cells are "D-shaped" with an irregular outline and have a low aspect ratio (Figure 5B) [42]. Examination of actin filament density along the front cell margin found this to be graded from the middle to sides of the cell. In fast moving cells, the ratio of actin filament density at the middle versus the sides was high but this was low in slow moving cells. Remarkably, 93% of all fan-shaped keratocytes could be described in terms of their area and aspect ratio. A 2D model of keratocyte motility was developed by Keren et al. [42], to relate cell shape and speed to actin filament dynamics [42]. Following on from the work of Grimm et al., 2002 [37], actin filament

actin filament density was assumed to be graded along the front edge and that the actin meshwork is stationary with respect to the substratum during protrusion [50]. To account for the conservation of cell area, it was proposed that the force generated by polymerizing actin at the leading edge is opposed by membrane tension. This was likened to the actin meshwork being enclosed in an inextensible "membrane bag", so that any increases in tension would be instantly equalized along the cell margin. Therefore, the net protrusive force at any given point along the front edge would depend on the density of the actin meshwork and membrane tension. According to this idea maximal rates of protrusion would occur at the middle of the front edge where actin filament density is highest, because the opposing membrane tension, per actin filament will be below the stall force for polymerization. As actin filament density decreases toward the sides of the cell, the load per filament increases until the stall force is reached and the rate of polymerization becomes zero. This relationship was quantified in a model that related actin filament dynamics and membrane tension to cell shape and speed. The model predicted that the majority of cell shape variation could be described by only two parameters, cell area, A and *z*. The parameter *z* is defined as: $z = T\gamma/f_{stall}\ \beta$, where γ = rate of capping of existing filaments, β = total number of daughter filaments that branch off existing growing ends, per second, and T = membrane tension. Since parameter *z* can represent the ratio of actin density between the middle and sides of the lamellipodium, it can also represent the cell's aspect ratio, and thus geometry. To relate cell shape to speed, the force velocity relationship for actin polymerization was obtained from studies of moving keratocytes and cytoplasmic extracts.

2.2.4. A 2D multiscale model of lamellipodial fragments

For decades, cell motility research has focused on the mechanism of protrusion, since the lamellipodium is considered to be the motile "organ" of the cell. This view was reinforced by finding that lamellar fragments obtained from keratocytes are autonomously motile, exhibiting a fan-shape and moving in a directed manner, similar to a whole cell [26]. Furthermore, the minimal molecular components for protrusion had recently been identified [56]. However, at the beginning of the 21st century an increasing number of models attempted to integrate other cytoskeletal functions besides protrusion, with movement of the cell as a whole. One of the first of these was proposed by Rubinstein et al., 2005 [43], who developed a 2D model of motility based on the movement of lamellar fragments. In addition to relating actin filament dynamics to the GRE model, this model incorporates adhesion strength, contractility and retraction to recapitulate the shape and motion of lamellar fragments, as follows. The rate of actin polymerization at the front edge is assumed to be limited by both the concentration of free G-actin or G-actin-profilin complexes, and the rate at which disassembled actin is transported to the front of the cell. The stability of new protrusions depends on adhesion to the substratum. In this model, the density of adhesions is highest at the front and decreases toward the rear. This gradient of adhesion density is modeled as being due to the increasing elastic deformation of the actin meshwork due to the activity of myosin II. Thus the density of F-actin and hence protrusion rate is graded along the leading edge until it, reaches a critical minimum, at which point the actin meshwork collapses into an actin-myosin bundle at the rear edge of the lamellipodium. The low F-actin density at the rear means that the local concentration of monomeric G-actin is relatively high so that diffusion and convection generate a gradient from the rear to the cell front, where it maintains a high rate of actin polymerization.

This model can reproduce keratocyte shape and constant, highly directed movement. It is noteworthy that this is achieved with a minimal set of motile sub processes. Further validation of this model came from its recapitulation of an experiment in which caged thymosin β4 was photoreleased on the left side of the cell, causing it to turn by pivoting in an anticlockwise direction around this point [57]. Upon the simulated release of thymosin β4 the free G-actin concentration drops on the left of the cell, so that protrusion and contraction are decreased on this side. Continued advance of the right side of the cell fragment causes it to pivot toward the left, at a similar rate to what is observed experimentally.

2.2.5. A 2D model for adhesion dependent shape determination in keratocytes

It has long been recognized that there is a biphasic relationship between cell speed and surface adhesiveness [58]. Cell speed is optimal at an intermediate level of adhesiveness but is inhibited when this is either too high or too low. In addition to the effects on cell speed, surface adhesiveness can have profound effects on the distribution, formation and dynamics of cytoskeletal structures such as stress fibers, and focal adhesions. For example, Ptk1 epithelial cells exhibit specific organizational states of myosin II, adhesion distribution and actin filament dynamics when attached to surfaces of low, medium and high adhesive strength [59]. Likewise, keratocyte shape and speed are also affected by changes in surface adhesiveness, and are accompanied by redistribution of myosin II and adhesions together with alterations in actin filament dynamics [44].

In this study, a mechanical model was developed to account for how the interaction between different motile sub-processes can lead to global changes in cell behavior. Briefly, the net rate of protrusion (or retraction) will depend on the interaction between polymerizing actin, membrane tension, the rate of retrograde flow and adhesion strength, which is represented as frictional drag opposing flow. The rate of protrusion or retraction was defined as $v(\mathrm{s}) = V\mathrm{p}(\mathrm{s}) + U\perp(\mathrm{s})$, where s is position along the cell boundary, V_p is the rate of actin polymerization, and $U_\perp$ is the component of centripetal bulk flow $\vec{U}$ of the actin meshwork (Figure 6). At s = 0, inset (a) the rate of actin polymerization is greater than retrograde flow, so that all the newly polymerized actin contributes to protrusion (grey arrow), which is maximal at this position. The actin cytoskeleton is stationary with respect to the substratum, because it is anchored to it via newly formed adhesion complexes, consisting of an actin binding protein (blue symbol) clutch proteins (striped symbol) and an adhesion receptor (cross-hatched symbol) bound to an extracellular matrix protein (red semicircle). Contractile forces (green arrow) and resulting retrograde flow are negligible, therefore traction stress (red arrows) is low, as is the resultant strain in the substratum (black arrow). At s = −50 and +50, inset (b) retrograde flow of actin (large green arrow) is equal to the rate of polymerization, therefore there is no net protrusion. The contractile forces are high, so that large traction stresses transmitted to the substratum, which experiences increased resultant strain (black arrows). High contractile stress at sites of adhesion causes them to mature and to slide or "rake" against the substratum, thus providing resistive force to retrograde flow. At inset (c) the rate of retrograde flow is greater than the rate of protrusion, however adhesions disassemble allowing the rear edge to detach and to retract (grey arrow). Although contractile forces are high, little of this is transmitted through disassembling adhesions, resulting in negligible traction stress, and resultant strain in the substratum.

The effect of varying adhesive strength on myosin II localization, adhesion distribution, retrograde flow and ultimately, cell shape and speed shape and speed was tested *in silico* by

changing the adhesion drag coefficient ζ, beneath the cell to low, medium and high (0.04, 0.2 and 20 nN $\times$ s/um^4, respectively). The simulation results closely matched experimental observations and predicted an adhesion dependent switch between mechanisms of cell shape determination.

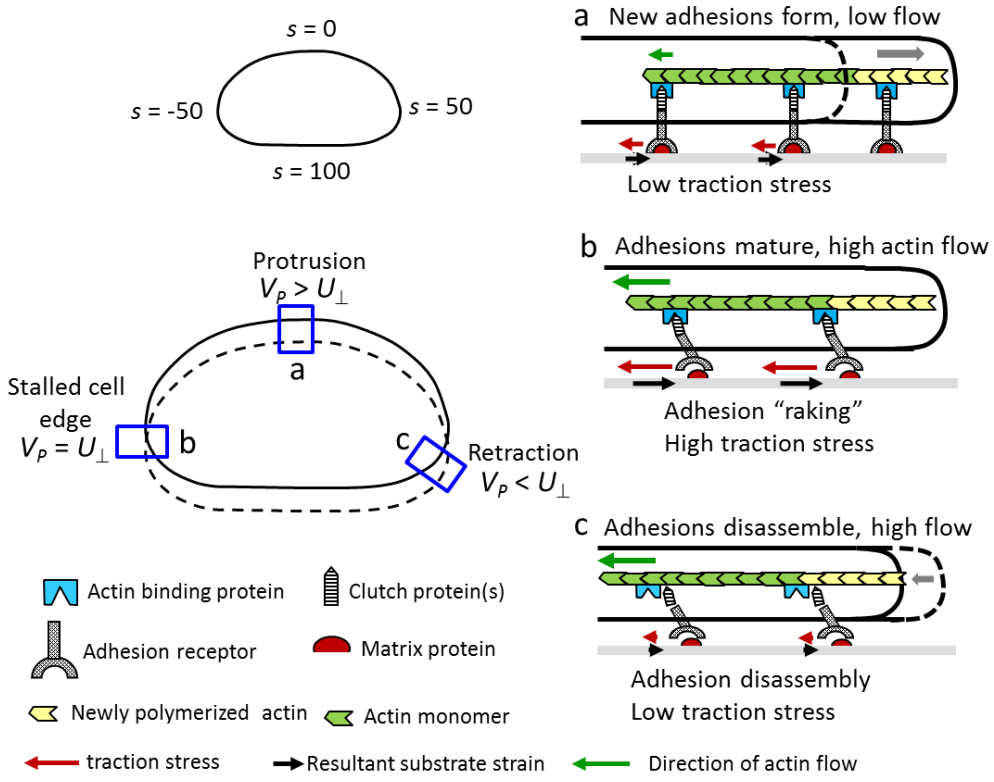

Figure 6. Diagram illustrating the relationship between actin filament dynamics, adhesion strength and traction stress at different positions (a–c) along the keratocyte cell margin. An outline of a keratocyte (top left) with positions marked at the front (s = 0) the left (s = −50), the right (s = 50) and back (s = 100) of the cell. Outline of a moving keratocyte (bottom left) where the rate of protrusion is: Greater than retrograde flow (a) equal to retrograde flow; (b) and less than retrograde flow. Insets (a–c) are diagrams of the side view of the lamellipodium corresponding to those indicated on the keratocyte cell outlines.

Experimental observations showed that cells attached to surfaces of low adhesiveness were more rounded had a low aspect ratio and moved slowly. In addition, adhesion complexes and myosin II were localized around the cell body. The simulation results revealed that the retrograde flow of actin is high, and graded along the front cell edge, so that myosin II and adhesions are swept inward toward the cell body (Figure 7A). Since adhesions are assumed to inhibit actin polymerization in this model, their relocation is thought to allow a high, constant rate of actin polymerization along the cell margin. The reason why cells are rounded and move slowly is because even though the actin polymerization rate is high, so is retrograde flow, thus limiting protrusive force generation. At intermediate adhesiveness, keratocytes exhibit a typical fan shape and have a high aspect ratio, which is associated with rapid movement. Experimental observations show mature adhesions and

myosin II concentrated at the rear. It was suggested that due to increased surface adhesiveness, myosin II is not swept inward but becomes concentrated at the cell rear, together with mature focal adhesions (Figure 7B). Since the presence of focal adhesions is assumed to inhibit actin polymerization, a decreasing polymerization rate is established between the front and sides of the cell, leading to graded rates of protrusion. At high levels of adhesiveness, cells are well spread but have a low aspect ratio and move slowly. Myosin II and mature adhesions fail to localize to the rear but are distributed throughout the cell (Figure 7C). Simulation results show that this organization of myosin II and adhesions is associated with a shallower gradient of actin polymerization rates between the middle and sides of the cell. Large focal adhesions close to the cell front are suggested to reduce actin polymerization rates, thus decreasing cell speed.

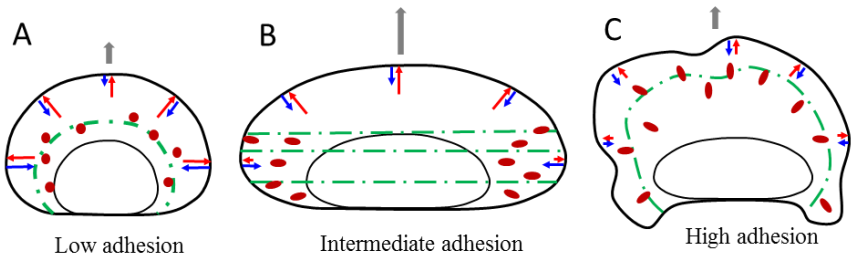

Figure 7. Diagrams summarizing the effect of altering substratum adhesiveness on the organization of adhesions, myosin II, actin polymerization and retrograde flow rates. A: On low adhesive substrata keratocytes are more rounded have a low aspect ratio and move slowly (small grey arrow). Retrograde flow is graded along the cell margin as indicated by the size and orientation of the blue arrows. Actin polymerization rate is high and constant along the cell margin as indicated by the size and orientation of the red arrows. Myosin II (green dot and dashed line) and adhesion sites (brown circles) are localized around the cell body. On substrata of intermediate adhesiveness keratocytes exhibit a typical fan shape have a high aspect ratio and move rapidly (large grey arrow). Retrograde flow rate is less than A and constant along the cell margin. Actin polymerization rate is high at the middle of the front edge and decreases toward the sides. Myosin II and mature adhesions (brown ovals) become localized toward the cell rear. On substrata of highest adhesiveness cell shape is rounded with a low aspect ratio, an irregular leading edge and move slowly (small grey arrow). Retrograde flow is the lowest and so is the actin polymerization rate. The ratio of actin polymerization at the front versus the sides is low. Reduced retrograde flow rates result in myosin II being distributed close to the cell front rather, and mature adhesions are distributed throughout the cell.

In all of the above simulations, the initial input of cell shape and speed were obtained from experimental observations, therefore it might not be surprising to obtain a good match between theory and experiment. It is noteworthy then, that the same result was obtained when a circular input shape was used for the simulations. Not only does this provide additional validation for the model, but demonstrates how cell shape and speed can emerge from the dynamic, physical interactions between the plasma membrane and cytoskeletal sub-processes such as actin polymerization, adhesion turnover and cytoskeletal contractility. This model also shows that

moving cells can readily adapt by "re-configuring" the distribution of cytoskeletal functions in response to environmental changes.

2.2.6. Cytopede: A 3D biomechanical model of cell movement

Most models of keratocyte consider the cell as a flat two-dimensional object, which is a reasonable approximation to make, considering that the cell's large lamellipodium is only ~0.2 μm in thickness. However, there is clearly a three dimensional aspect to keratocyte movement, as reflected by the circumferential motion of lamellar ridges. In addition, the retrograde flow of ruffles on the dorsal surface of fibroblasts is well-documented. The first three-dimensional model of keratocyte and fibroblast motility was developed by Herant and Dembo in 2010 [35]. This model links the material properties of the cytoskeleton and its biochemistry to the mechanics of cell movement. The model consists of a low-Reynolds number hydrodynamic finite element code, named "Cytopede". The cell is assumed to be a viscoelastic body where the cytoplasm consists of two-fractions; a fluid viscous cytosol and a solid, viscoelastic cytoskeleton. These are modeled as a two-phase interpenetrating flow for which the velocity field for each fraction is determined at every point within the cell. Actin polymerization and depolymerization are represented by the interconversion between a liquid cytosol and a solid cytoskeleton. The material properties of the cytoskeleton such as rigidity can be changed by varying the degree of crosslinking. The model also incorporates surface stresses due to membrane tension and the dynamics of adhesion peeling from the substrate.

Simulation of cell movement for either a fibroblast or keratocyte begins with a hemispherical cell that flattens and spreads upon the substratum. To simulate spreading, the model has to invoke a vertical contractile force that together with actin polymerization squeezes and pushes the cell margin outward. As the cell flattens, its area and surface tension increase, which resists protrusion, until an equilibrium is reached. Simulation of keratocyte movement begins from the spread state after a polymerization signal is activated along 50% of the cell margin (Figure 8A). Following initiation of protrusion at the cell front, hydrodynamic pressure pushes the lateral edges out but this is opposed by viscous forces and restrained by surface tension. When an equilibrium is reached the cell is ~30 μm in width, ~10 μm in length and moving at a rate of 0.1 μm/s in agreement with experimental observations of keratocytes. Since the lateral edges cannot advance, polymerizing actin is forced rearward, resulting in a high rate of retrograde flow in these regions, similar to what has been observed using fluorescence speckle microscopy [60–62]. This leads to high vertical shear that is transmitted to the substratum at either side of the keratocyte, and corresponds to the regions where high inward directed traction stresses have been detected [63]. To conserve cell area the rear edge is pulled forward and retraction occurs when the critical contact angle for detachment is less than 80 °. At steady-state, the shape and rapid gliding mode of simulated keratocyte movement are almost identical to real keratocytes. In addition, the kinematics of the predicted cytoskeletal flow field is very similar to that of the GRE model.

Remarkably, simulation of fibroblast movement results from altering only two parameters, the activation of protrusion along 25% of the cell margin and setting the critical contact angle for detachment to <45 ° (Figure 8B). Following the onset of movement, the simulated cell elongates in the direction of movement, stretching the rear out into a "tail". The resultant morphology and speed are strikingly similar to the triangular shape of a fibroblast, being ~30 μm long and moving at 0.03 μm/s. For both the simulated fibroblast and keratocyte, mechanical coupling between the

front and rear of the cell is mediated by membrane tension. Therefore, as protrusion occurs the rear is pulled forward, however, in the keratocyte rate of actin disassembly must be increased by ten times along the non protruding edges of the cell, to prevent a large tail from forming due to the accumulation of cytoplasm at the rear.

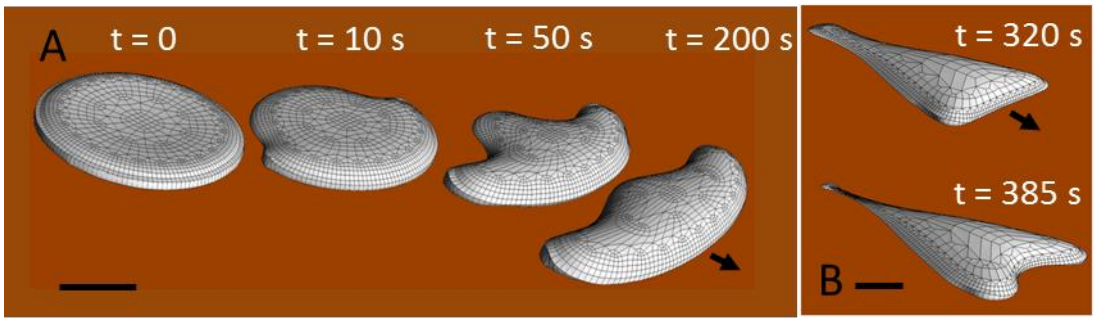

Figure 8. Simulation of keratocyte and fibroblast movement using *Cytopede*. A: A three dimensional rendering of the cell surface of simulated keratocyte movement starting from a flattened discoid shape (t = 0). Protrusion is allowed along 50% of the cell margin (t = 10 s) then a keratocyte-shape emerges (t = 50 s) with a trailing rear end. The passive rear is stretched between the two lateral edges of the keratocyte as it acquires steady-state shape and motion. Surface lines correspond to the computational mesh. B: Simulation of fibroblast movement from an initial discoid shape as shown in A, in which polymerization occurs along 25% of the cell margin. Still images of the simulation show a typical fibroblast shape at t = 320 s that develops a thin tail at the rear and a bilobed leading edge at t = 385 s. Scale bars = 10 μm. Panels A and B are reproduced with permission from M. Dembo.

2.2.7. The use of minimal models to determine the redundant mechanisms underlying keratocyte movement

The presumption underlying this work is that cell motility is a self-organizing system that emerges from the combined activities of a number of motile sub-processes. One characteristic of a self-organizing system is that it is robust, due to the existence of redundant mechanisms [64]. The goal of the following work was to determine whether a single sub-motile process or a combination thereof could recapitulate keratocyte motility [45]. Four different minimal models were developed, using the moving-boundary (level-set) method and assessed with respect to their ability to reproduce a realistic shape and mode of keratocyte movement. The four minimal models were based on G-actin transport, microtubule associated vesicle transport, Rho GTPases, and myosin II dependent contractile force generation. Although the first three models could reproduce keratocyte movement, only the first and last of these will be discussed here.

The premise of the G-actin transport model is that protrusion is limited by the rate at which G-actin monomers diffuse from a depolymerization zone at the rear, to the cell front and sides where actin filament growth occurs. The simulation begins with a circular cell and a uniform concentration of G-actin. As actin polymerization occurs at the front, it depletes the source of G-actin here, leading to protrusion. Meanwhile, disassembly further back increases the pool of G-actin, and since the sides

of the cell are closer to this region than the leading edge, they protrude outward causing the cell to widen. To conserve cell area, the rear is pulled forward, bringing the depolymerizing zone closer to the front, allowing polymerization to occur faster here than at the sides. This simulation results in a realistic fan-shaped cell, moving at a constant velocity.

In the myosin II contractility model, the actin cytoskeleton was assumed to behave as a viscous fluid, to which myosin II could bind or unbind at specified rates. When bound to actin, myosin II is modeled to generate isotropic stress in the cytoskeleton that is proportional to its local concentration. As a result, the actin meshwork flows inward together with the bound myosin II causing it to become concentrated at the rear. Adhesions are modeled as sites that generate a resistive drag force, since they oppose retrograde actin flow. Actin polymerization is assumed to occur along the cell edge, and decreases in proportion to the increasing concentration of myosin II toward the rear. Surprisingly, this model did not reproduce keratocyte movement, even though a variety of cell shapes could form in response to a range of permutations in the model parameters. However, keratocyte movement could only be reproduced if graded rates of treadmilling actin were assumed to exist at the front of the cell.

The fact that different minimal models can reproduce keratocyte motility supports the idea that it is robust. However, in reality protrusion is not limited by G-actin transport. This is because much of it is sequestered by Thymosin β-4 or exists as an actin-profilin complex at the leading edge, which can readily fuel the growth of actin filaments. Failure of the myosin II model to reproduce keratocyte movement suggests that it is not a redundant mechanism. In agreement with this, many studies have shown that cell movement is impaired when myosin II is inhibited or knocked out.

2.2.8. Modeling the movement of amoeboid sperm from Ascaris suum: Another "fan-shaped" cell type

A remarkable example of parallel evolution is the similarity of shape and mode of movement between the amoeboid sperm from the nematode, *Ascaris suum* and fish epithelial keratocytes (Figure 9) [65]. Even more remarkable is the fact that *Ascaris* sperm movement occurs independently of actin and associated proteins. Instead it is powered by the assembly and disassembly of major sperm protein (MSP) filaments. Despite possessing a non-actin containing cytoskeleton *Ascaris* sperm exhibit the same directed movement and constant fan shape as keratocytes. In 2001, Bottino et al., developed a finite element model of *Ascaris* motility based on the biochemistry of MSP, which recapitulated their keratocyte-like motility [46].

The cytoskeleton of *Ascaris* sperm assembles from subunits into helical subfilaments that wind together to form larger filaments. These interact laterally with each other to form even larger, branched multifilament meshworks, or fiber complexes that span the length of the lamellipod. MSP filaments grow by the addition of MSP subunits at the front cell edge and disassemble at the rear, just in front of the nucleus in the perinuclear zone. As with actin filaments, polymerization at the front generates a protrusive force but the molecular mechanism differs. As MSP subunits polymerize, the filaments bind laterally, which stretches the filament and holds it in place, generating a protrusive force. It has been proposed that elastic energy is stored in the filaments in their stretched conformation so that when MSP filaments disassemble elastic energy is released as they relax back to their original length. This generates a contractile force that pulls the rear forward. Spatial regulation of protrusion and retraction is controlled by a pH gradient, whereby a more alkaline pH at

the front favors assembly, while acidic conditions at the rear favor disassembly. A conceptual model has described this as the "push-pull" mechanism of *Ascaris* movement [47].

Figure 9. Similarities in shape between the amoeboid sperm of *Ascaris suum* and a fish epithelial keratocyte. A: A differential interference contrast image of the amoeboid sperm of *Ascaris*, moving in the direction indicated (arrow). Note the flat, fan-shaped lamellipodium at the front and bulbous cell body at the rear. B: A phase contrast image of a moving fish epithelial keratocyte. Note its similar morphology to the cell in A. Scale bars = 5 μm. The image in A was provided by courtesy of J. Italiano.

In the 2D model of *Ascaris* sperm movement the lamellepod is represented by a mesh of triangular elements, or Voronoi polygons, and nodes at each vertex [46]. During protrusion new nodes are introduced to represent polymerization and bundling of MSP. To represent protrusive force, a load-velocity relationship for edge advancement is used to calculate a pressure, normal to the cell boundary (detailed in the appendix). The process of retraction is mimicked, by removing rearmost nodes as they approach acidic regions of the cytosol during forward motion, and is modeled by subtracting tensile stress and adhesive drag force from this node. This allows the simulated MSP fibers to detach from the substratum and relax back to their original rest length. Cell substratum adhesion sites are represented by a frictional drag force that acts to oppose node movement. An important feature of this model is that adhesion strength is modeled to be higher at the cell front than at the rear. Therefore, when disassembly occurs at the rear, a node will be pulled toward the front of the cell, rather than the rear. Validation of the model is given by its replication of the cell's response both to changes in intracellular pH, and increases in substratum adhesiveness. For example, by increasing the adhesive drag under the cell body, the effect of increasing cell-substratum adhesiveness can be mimicked. In the both the simulation and real cells a reduction of cell speed occurs, together with an increase in cytoskeletal retrograde flow.

One of the major insights provided by this model is that the biochemical identity of the cytoskeleton is less important than the pattern of force generation, as long as this is the same as that produced by an actin containing cytoskeleton. A second insight is that *Ascaris* movement is robust, since changes in some of the mechanical and kinetic parameters of the model do not cause any significant changes in simulated cell shape.

2.2.9. A "top-down" model that reproduces the shape and movement of different cell types

A single cell type can exhibit different shapes and modes of movement depending on environmental cues [66]. For example, some keratocytes can switch from a gliding, fan-shaped mode of movement to one in which they resemble fibroblasts, when they are attached to an adhesive surface [67]. Conversely, other cell types can exhibit a keratocyte-like "fan" shape during rapid movement, such as HT1020 fibrosarcoma cells [68], rat bladder carcinoma cells [69] and amiB-null mutants of *Dictyostelium discoideum* [70]. The fact that the key molecular mechanisms involved in movement are the same for all motile eukaryotic cells suggests that various modes of movement arise from differences in the way these mechanisms are coordinated with each other. This possibility was explored by the "top-down" model developed by Satulovsky et al. [36]. The model is based on the local stimulation, global inhibition model that has previously been used to model chemotaxis in leukocytes [71]. It is assumed that a local positive feedback promotes protrusion at the front, while it is inhibited globally. Simulations of cell movement were made using a circular "shape machine" in which points along the circumference move outwards, to represent protrusion, or inward to represent retraction, in response to the balance of a local protrusion and global retraction signals. The magnitude of these signals was represented by the length of the radius connecting the centroid with a point on the perimeter of the circle. At each time point, the centroid of the cell is recalculated according to magnitude of protrusions and retractions. This model also includes deterministic rules that control signals, such as their generation and decay rate, together with stochastic signals that influence the cell's turning frequency. A set of metrics, such as cell area, fluctuations in area, cell roundness, speed and persistence were used to compare the results of simulations with experimental observations. These comparisons were used to determine which model parameters best match those obtained from real cells. Surprisingly, hundreds of model parameter combinations could simulate *Dictyostelium* movement. This suggests that the "control circuits" of cell motility are robust and that compensatory mechanisms act to maintain a particular mode of movement. Analysis of the relationships between different sets of model parameter alterations and the associated simulated cell metrics allowed determination of the relative importance that each parameter has on the generation of cell shape. This approach was used to make "mathematical mutations" by altering each model parameter and observing how this affects simulated *Dictyostelium* movement. For example, adding adhesion sites to the *Dictyostelium* simulation resulted in a cell, shaped like a fibroblast that exhibited the same discontinuous mode of movement. Interestingly, increasing local positive feedback control over protrusion resulted in a simulated cell resembling a keratocyte, with a large lamellipodium and a constant, highly directed mode of movement.

3. Discussion

The models of motility discussed here have all contributed to our understanding of motility, in some way. Conceptual models are useful as a means of visualizing a particular process and for forming initial hypotheses. 1D models can provide a course-grained understanding of a specific process. For example, the model developed by Grimm et al., 2003 [37] shows how Arp2/3 mediated actin filament branching, and the activity of actin filament capping proteins can shape the lamellipodium. More complex, multi-scale 2D and 3D models are important both for integrating molecular processes at the cellular level, and for studying how changes in specific molecular

interactions can effect movement. Furthermore, simpler models often provide a foundation for a more complex one. For example, the model of Grimm et al., 2003 [37], formed the basis for the model of keratocyte shape generation developed by Keren et al., 2008 [42], and this was developed further by Barnhart et al., 2011 [44]. The collective insight provided by these multiscale models is that cell motility is a self-organizing system that emerges from the dynamic balance between forces that tend to push the membrane out and those that pull it inward. We have seen that this is accomplished through the mechanical interaction and feedback regulation between key sub-processes of motility.

The validity of the multiscale models discussed here is generally tested by seeing if they can reproduce keratocyte shape and movement. This is not simply a means of mimicking keratocyte movement but is a necessary first step before using the model to test hypotheses, or to examine the effect of altering certain parameters on cell shape and speed. For example, Barnhart et al., 2011 [44] used their model of keratocyte motility to test the effects of varying substratum adhesiveness.

The combination of experimentation and modeling has provided some answers to the question of how molecular mechanisms are integrated at the cellular level, in addition to raising some new ones. For instance, at the front of the cell, graded rates of protrusion are the net result of the "pushing" force generated by the polymerizing actin meshwork and the opposing load of the plasma membrane. However, since membrane tension is constant along the cell margin, it cannot provide any spatial control over the rate of polymerization. Instead, positional information is provided by the decreasing gradient of actin filament density from the middle to the sides of the lamellipodium. Nevertheless, the question remains as to how this is established in the first place. One possibility is that the localization of myosin II dependent contractile forces at the rear could induce an increase actin filament disassembly [61]. Alternatively, large myosin II-dependent retrograde flow rates could subtract newly polymerized actin from the adjacent edge, thus reducing protrusive force. Both scenarios are plausible, since large traction forces are found at the lateral rear edges of keratocytes. The existence of focal adhesion-like structures at the rear means that the resistance to retrograde flow will be particularly high in these regions, especially at the ventral cell surface. It is of interest that the model of keratocyte motility developed by Herant and Dembo, 2010 [35] predicted that large vertical shear forces exist at the rear lateral edges. Therefore, it is possible that these shear forces "thin-out" the actin meshwork, reducing its density toward the rear.

A common feature of the multiscale models described here is that adhesions are modeled as being stronger at the front to promote protrusion, whereas contractile forces are modeled as being higher at the rear, to facilitate retraction. In addition, this spatial distribution of adhesiveness and contractility is dynamic, allowing cell movement to resume after perturbation [42] or to be "re-configured" depending on changes in extracellular conditions, such as substratum adhesiveness [44]. This raises the question of how such a pattern of contractile forces is established and maintained. The first step is the development of polarity [27], which since keratocytes are not chemotactic, begins with an increase in contractility at the presumptive rear of the cell [72] and like the most cell types involves the activation of the Rho GTPases [27]. However, a remaining question concerns how the inverse gradients of contractile force and adhesion strength arise. One possibility is that the self-organizing activity of myosin II generates the increasing gradient of contractile force toward the cell rear that progressively weakens adhesions until they allow detachment to occur at the rear. A similar assumption was made in the multiscale model of Rubenstein et al. [43]. Another possibility is that the same average level of adhesiveness exists beneath the entire cell but the

increasing gradient of contractile force induces retraction, when it supersedes adhesive forces at the rear. A third possibility is that the self-organization of myosin II distribution and the mechanosensory response of adhesions to force determine the strength of adhesions relative to contractile force. Although adhesions are considered to be stronger at the front than at the cell rear, experimental observations of adhesions and traction stresses in keratocytes suggest the opposite. The largest adhesions [44,73,74] and traction stresses [63] are found at the lateral rear edges of keratocytes. A solution to this paradox is that it is the relative strength of adhesions to contractile force that is important not their absolute strength. Thus small focal complexes beneath the leading edge strengthen in response to weak contractile forces at the cell front. Here, adhesive forces predominate as nascent adhesions begin to "grip" the substrate, generating propulsive tractions (Figure 6A) [53]. At the lateral rear edges, mature focal adhesions that are under the most stress begin to slip inward with respect to the substratum, which generates larger traction stresses here (Figure 6B), but also triggers adhesion disassembly (Figure 6C) [75]. Both experimental observations [62] and modeling adhesions in "gripping" and "slipping" modes [76] support this idea. From the above one may conclude that myosin II generated contractile forces are necessary and sufficient for organizing the rates of protrusion and retraction along the cell margin, if the mechanosensory response of adhesions is taken into account.

4. Future directions

The relative simplicity of keratocyte movement will ensure that it continues to be the subject of experimental and modeling efforts. Multiscale modeling has provided insight into the integration of cytoskeletal function, however another recent modeling approach involves the development of minimal "modular" models of motility [77]. These models use phase-field approach to solve the moving boundary problem associated with cell movement. This offers a promising new approach for studying the mechanism of motility, because it allows an incremental increase in model complexity by adding different modules. For example, an additional module may be added to consider substrate elasticity, so that the pattern of traction stresses and substrate deformation can be considered. Likewise, the movement of different cell types may be modeled by tailoring an "actin dynamics" module to a specific cell type. It is possible that modular modeling will be particularly well suited for the integration of biomechanical mechanisms across multiple size scales.

Thus far most models of keratocyte motility have centered on the constant, steady-state movement of these cells, and yet experimental work has shown that they exhibit spontaneous turns, circling trajectories and oscillations [12,78]. They may move with a "waddling" bipedal motion [79] or in a discontinuous manner resembling fibroblasts [67]. Understanding the how the transition between these types of movement occurs will shed light on the plasticity of movement in general, which is relevant to the epithelial to mesenchymal transition that is at the heart of cancer metastasis [80]. Studies along these lines have already shown that small changes in key parameters can switch a fibroblastic movement to that of keratocytes [35] and that amoeboid movement can likewise be transformed to a variety of cell types [36]. In addition to understanding its basic mechanism(s), another major goal of cell motility research is to learn how movement occurs in a 3D environment. Therefore, the combined approach of mathematical modeling and experimentation will continue to reveal new insights as cell motility research moves into this new frontier.

Acknowledgements

The author thanks Dr. A Albert for her advice and encouragement.

Conflict of interest

The author declares no conflict of interest in this paper.

References

1. Pollard TD, Borisy GG (2003) Cellular motility driven by assembly and disassembly of actin filaments. *Cell* 112: 453–465.
2. Pollard TD (2003) The cytoskeleton, cellular motility and the reductionist agenda. *Nature* 422: 741–745.
3. Holmes WR, Edelsteinkeshet L (2012) A comparion of computational models for eukaryotic cell hape and motility. *PLoS Comput Biol* 8: e1002793.
4. Danuser G, Allard J, Mogliner A (2013) Mathematical modeling of eukaryotic cell migration: Insights beyond experiments. *Annu Rev Cell Dev Biol* 29: 501–528.
5. Mogiler A (2009) Mathematics of cell motility: Have we got its number? *J Math Biol* 58: 105–134.
6. Mogilner A, Keren AK (2009) The shape of motile cells. *Curr Biol* 15: 762–771.
7. Oelz D, Schmeiser C (2011) Simulation of lamellipodial fragments. *J Math Biol* 64: 513–528.
8. Adler Y, Givli S (2013) Closing the loop: Lamellipodia dynamics from the perspective of front propagation. *Phys Rev E* 88: 042708.
9. Recho P, Putelat T, Truskinovsky L (2013) Contraction-driven cell motility. *Phys Rev Lett* 111: 108102.
10. Tjhung E, Tiribocchi A, Marenduzzo D, et al. (2015) A minimal physical model captures the shapes of crawling cells. *Nat Commun* 6: 5420.
11. Ambrosi D, Zanzottera A (2016) Mechanics and polarity in cell motility. *Physica D* 330: 58–66.
12. Raynaud F, Ambühl ME, Gabella C, et al. (2016) Minimal models for spontaneous cell polarization and edge activity in oscillating, rotating and migrating cells. *Nat Phys* 12: 367–374.
13. Pollard TD, Cooper JA (2009) Actin, a central player in cell shape and movement. *Science* 326: 1208–1212.
14. Rafelski SM, Theriot JA (2004) Crawling toward a unified model of cell motility: Spatial and temporal regulation of actin dynamics. *Annu Rev Biochem* 73: 209–239.
15. Mogilner A (2006) On the edge: Modeling protrusion. *Curr Opin Cell Biol* 18: 32–39.
16. Svitkina TM, Verkhovsky AB, Mcquade KM, et al. (1997) Analysis of the actin-myosin II system in fish epidermal keratocytes: Mechanism of cell body translocation. *J Cell Biol* 139: 397–415.
17. Clainche CL, Carlier MF (2008) Regulation of actin assembly associated with protrusion and adhesion in cell migration. *Physiol Rev* 88: 489–513.
18. Vincente-Manzaneres M, Choi CK, Horwitz AR (2009) Integrins in cell migration—the actin connection. *J Cell Sci* 122: 199–206.
19. Gardel ML, Schneider IC, Aratyn-Schaus Y, et al. (2010) Mechanical integration of actin and adhesion dynamics in cell migration. *Annu Rev Cell Dev Biol* 26: 315–333.

20. Suter DM, Forscher P (2000) Substrate-cytoskeletal coupling as a mechanism for the regulation of growth cone motility and guidance. *Dev Neurobiol* 44: 97–113.
21. Vincente-Manzaneres M, Ma X, Adelstein RS, et al. (2009) Non-muscle myosin II takes centre stage in cell adhesion and migration. *Nat Rev Mol Cell Biol* 10: 788–790.
22. Kirfel G, Rigort A, Borm B, et al. (2004) Cell migration: Mechanisms of rear detachment and the formation of migration tracks. *Eur J Cell Biol* 83: 717–724.
23. Lee J, Ishihara A, Oxford G, et al. (1999) Regulation of cell movement is mediated by stretch-activated calcium channels. *Nature* 400: 382–386.
24. Huttenlocher A, Palecek SP, Lu Q, et al. (1997) Regulation of cell migration by the calcium-dependent protease calpain. *J Biol Chem* 272: 32719–32722.
25. Wolfenson H, Bershadsky A, Henis Y, et al. (2011) Actomyosin-generated tension controls the molecular kinetics of focal adhesions. *J Cell Sci* 124: 1425–1432.
26. Verkhovsky AB, Svitkina T, Borisy GG (1999) Self-polarization and directional motility of cytoplasm. *Curr Biol* 9: 11–20.
27. Ridley AJ, Horwitz AR (2003) Cell migration: Integrating signals from front to back. *Science* 302: 1704–1709.
28. Friedl P, Sahai E, Weiss S, et al. (2012) New dimensions in cell migration. *Nat Rev Mol Cell Biol* 13: 743–747.
29. Lo CM, Wang HB, Dembo M, et al. (2000) Cell movement is guided by the rigidity of the substrate. *Biophys J* 79: 144–152.
30. Abercrombie M (1961) The bases of locomotory behaviour of fibroblasts. *Exp Cell Res* 8: 188.
31. Allan RB, Wilkinson PC (1978) A visual analysis of chemotactic and chemokinetic locomotion of human neutrophil leukocytes. *Exp Cell Res* 111: 191–203.
32. Lee J, Ishihara A, Jacobson K (1993) The fish epidermal keratocyte as a model system for the study of cell locomotion. *Symp Soc Exp Biol* 47: 73–89.
33. Tranquillo RT, Lauffenburger DA, Zigmond SH (1988) A stochastic model for leukocyte random motility and chemotaxis bases on receptor binding fluctuations. *J Cell Biol* 106: 303–309.
34. Mogilner A, Verzi DW (2003) A Simple 1-D physical model for the crawling nematode sperm cell. *J Stat Phys* 110: 1169–1189.
35. Herant M, Dembo M (2010) Form and function in cell motility: From fibroblasts to keratocytes. *Biophys J* 98: 1408–1417.
36. Satulovsky J, Lui R, Wang Yl (2008) Exploring the control circuit of cell migration by mathematical modeling. *Biophys J* 94: 3671–3683.
37. Grimm HP, Verkhovsky AB, Mogilner A, et al. (2003) Analysis of actin dynamics at the leading edge of crawling cells: Implications for the shape of the keratocyte lamellipodia. *Eur Biophys J* 32: 563–577.
38. Hellewell SB, Taylor DL (1979) The contractile basis of amoeboid movements. VI. The solation-contraction coupling hypothesis. *J Cell Biol* 83: 633–648.
39. Chen WT (1979) Induction of spreading during fibroblast movement. *J Cell Biol* 81: 684–691.
40. Harris A, Dunn G (1972) Centripetal transport of attached particles on both surfaces of moving fibroblasts. *Exp Cell Res* 73: 519–523.
41. Lee J, Ishihara A, Teriot JA, et al. (1993) Principles of locomotion for simple-shaped cells. *Nature* 362: 167–171.

42. Keren K, Pincus Z, Allen GM, et al. (2008) Mechanism of shape determination in motile cells. *Nature* 453: 475–480.
43. Rubenstein B, Jacobson K, Moglilner A (2005) Multiscale two-dimensional modeling of a motile simple-shaped cell. *Multiscale Model Sim* 3: 413–439.
44. Barnhart EL, Lee KC, Keren K, et al. (2011) An adhesion-dependent switch between mechanisms that determine motile cell shape. *PLoS Biol* 9: 1–16.
45. Wolgemuth C, Stajic J, Mogliner A (2011) Redundant mechanisms for stable cell locomotion revealed by minimal models. *Biophys J* 101: 545–553.
46. Bottino D, Moglilner A, Roberts T, et al. (2001) How nematode sperm crawl. *J Cell Sci* 115: 367–384.
47. Roberts T, Stewart M (2000) Acting like actin: The dynamics of the nematode major sperm protein (MSP) cytoskeleton indicate a push-pull mechanism for amoeboid cell motility. *J Cell Biol* 149: 7–12.
48. Janson LW, Kolega J, Taylor DL (1991) Modulation of contraction by gelation/solation in a reconstituted motile model. *J Cell Biol* 114: 1005–1015.
49. Forscher P, Smith SJ (1988) Actions of cytochalasins on the organization of actin filaments and microtubules in a neuronal growth cone. *J Cell Biol* 107: 1505–1516.
50. Theriot JA, Mitchison TJ (1991) Actin microfilament dynamics in locomoting cells. *Nature* 352: 126–131.
51. Harris AK, Wild P, Stopal D (1980) Silicone rubber substrata: A new wrinkle in the study of cell locomotion. *Science* 208: 177–179.
52. Wang JHC, Shang JS (2007) Cell traction force and measurement methods. *Biomech Model Mechan* 6: 361–371.
53. Beningo KA, Dembo M, Kverina I, et al. (2001) Nascent focal adhesions are responsible for the generation of strong propulsive forces in migrating fibroblasts. *J Cell Biol* 153: 881–887.
54. Hind LE, Dembo M, Hammer DA (2015) Macrophage motility is driven by frontal-towing with a force magnitude dependent on substrate stiffness. *Integr Biol* 7: 447–453.
55. Doyle A, Marganski W, Lee J (2004) Calcium transients induce spatially coordinated increases in traction force during the movement of fish keratocytes. *J Cell Sci* 117: 2203–2214.
56. Loisel TP, Boujemaa R, Pantaloni D, et al. (1999) Reconstitution of actin-based motility of *Listeria* and *Shigella* using pure proteins. *Nature* 401: 613–616.
57. Roy P, Rajfur Z, Jones D (2001) Local photorelease of caged thymosin beta 4 in locomoting keratocytes causes cell turning. *J Cell Biol* 153: 1035–1047.
58. DiMilla PA, Barbee K, Lauffenburger DA (1991) Mathematical model for the effects of adhesion and mechanics on cell migration speed. *Biophys J* 60: 15–37.
59. Gupton SL, Waterman-Storer CM (2006) Spatiotemporal feedback between actomyosin and focal-adhesion systems optimizes rapid cell migration. *Cell* 125: 1361–1374.
60. Jurado C, Haserick JR, Lee J (2005) Slipping or gripping? Fluorescent speckle microscopy in fish keratocytes reveals two different mechanisms for generating a retrograde flow of actin. *Mol Biol Cell* 16: 507–518.
61. Wilson CA, Tsuchida MA, Allen GM, et al. (2010) Myosin II contributes to cell-scale actin network treadmilling through network disassembly. *Nature* 465: 373–377.
62. Fournier MF, Sauser S, Ambrosi D, et al. (2010) Force transimission in migrating cells. *J Cell Biol* 188: 287–297.

63. Lee J, Leonard M, Oliver T, et al. (1994) Traction forces generated by locomoting keratocytes. *J Cell Biol* 127: 1957–1964.
64. Hartwell LH, Hopfield JJ, Leibler S, et al. (1999) From molecular to modular cell biology. *Nature* 402: C47–C52.
65. Italiano JE, Stewart M, Roberts TM (2001) How the assembly dynamics of the nematode major sperm protein generate amoeboid cell motility. *Int Rev Cytol* 202: 1–34.
66. Friedl P, Wolf K (2010) Plasticity of cell migration: A multiscale tuning model. *J Cell Biol* 188: 11–19.
67. Doyle AD, Lee J (2005) Cyclic changes in keratocyte speed and traction stress arise from Ca^{2+}-dependent regulation of cell adhesiveness. *J Cell Sci* 118: 369–379.
68. Paku S, Tóvári J, Lörincz Z, et al. (2003) Adhesion dynamics and cytoskeletal structure of gliding human fibrosarcoma cells: A hypothetical model of cell migration. *Exp Cell Res* 290: 246–253.
69. Huang C, Rajfur Z, Borchers C, et al. (2003) JNK phosphorylates paxillin and regulates cell migration. *Nature* 424: 219–223.
70. Asano Y, Mizuno T, Kon T, et al. (2004) Keratocyte-like locomotion in amiB-null Dictyostelium cells. *Cell Motil Cytoskel* 59: 17–27.
71. Ma L, Janetopoulos C, Yang L, et al. (2004) Two complementary, local excitation, global inhibition mechanisms acting in parallel can explain the chemoattractant-induced regulation of PI(3,4,5)P-3 response in *Dictyostelium* cells. *Biophys J* 87: 3764–3774.
72. Yam PT, Wilson CA, Ji L, et al. (2007) Actin-myosin network reorganization breaks symmetry at the cell rear to spontaneously initiate polarized cell motility. *J Cell Biol* 178: 1207–1221.
73. Lee J, Jacobson K (1997) The composition and dynamics of cell-substratum adhesions in locomoting fish keratocytes. *J Cell Sci* 110: 2833–2844.
74. Anderson KI, Cross R (2000) Contact dynamics during keratocyte motility. *Curr Biol* 10: 253–260.
75. Morin TR, Ghassemzadeh SA, Lee J (2014) Traction force microscopy in rapidly moving cells reveals separate roles for ROCK and MLCK in the mechanics of retraction. *Exp Cell Res* 326: 280–294.
76. Shao D, Levine H, Rappel WJ (2012) Coupling actin flow, adhesion, and morphology in a computational cell motiliy model. *PNAS* 109: 6851–6856.
77. Ziebert F, Aranson IS (2014) Modular approach for modeling cell motility. *Eur Phys J-Spec Top* 223: 1265–1277.
78. Camely BA, Zhao Y, Li B, et al. (2017) Crawling and turning in a minimal reaction-diffusion cell motility model: Coupling cell shape and biochemistry. *Phys Rev E* 95: 012401.
79. Barnhart EL, Allen GM, Julicher F, et al. (2010) Bipedal locomotion in crawling cells. *Biophys J* 98: 933–942.
80. Sanz-Morena V, Gadea G, Paterson H, et al. (2008) Rac activation and inactivation control plasticity of tumor cell movement. *Cell* 135: 510–523.